Dual inhibition of cyclooxygenase-2 and soluble epoxide hydrolase synergistically suppresses primary tumor growth and metastasis

Guodong Zhang[a,b,1], Dipak Panigrahy[c,d,1], Sung Hee Hwang[a], Jun Yang[a], Lisa M. Mahakian[e], Hiromi I. Wettersten[f], Jun-Yan Liu[a], Yanru Wang[a], Elizabeth S. Ingham[e], Sarah Tam[e], Mark W. Kieran[g,h], Robert H. Weiss[f,i], Katherine W. Ferrara[e], and Bruce D. Hammock[a,2]

[a]Department of Entomology and Nematology and Comprehensive Cancer Center, University of California, Davis, CA 95616; [b]Department of Food Science, University of Massachusetts-Amherst, Amherst, MA 01003; [c]Center for Vascular Biology Research and [d]Department of Pathology, Beth Israel Deaconess Medical Center, Harvard Medical School, Boston, MA 02115; [e]Department of Biomedical Engineering, and [f]Division of Nephrology, Department of Internal Medicine, University of California, Davis, CA 95616; [g]Division of Pediatric Oncology, Dana–Farber Cancer Institute, and [h]Department of Pediatric Hematology/Oncology, Boston Children's Hospital, Harvard Medical School, Boston, MA 02115; and [i]US Department of Veterans Affairs Medical Center, Sacramento, CA 95655

Contributed by Bruce D. Hammock, June 12, 2014 (sent for review April 1, 2014; reviewed by Kenneth Honn)

Prostaglandins derived from the cyclooxygenase (COX) pathway and epoxyeicosatrienoic acids (EETs) from the cytochrome P450/soluble epoxide hydrolase (sEH) pathway are important eicosanoids that regulate angiogenesis and tumorigenesis. COX-2 inhibitors, which block the formation of prostaglandins, suppress tumor growth, whereas sEH inhibitors, which increase endogenous EETs, stimulate primary tumor growth and metastasis. However, the functional interactions of these two pathways in cancer are unknown. Using pharmacological inhibitors as probes, we show here that dual inhibition of COX-2 and sEH synergistically inhibits primary tumor growth and metastasis by suppressing tumor angiogenesis. COX-2/sEH dual pharmacological inhibitors also potently suppress primary tumor growth and metastasis by inhibiting tumor angiogenesis via selective inhibition of endothelial cell proliferation. These results demonstrate a critical interaction of these two lipid metabolism pathways on tumorigenesis and suggest dual inhibition of COX-2 and sEH as a potential therapeutic strategy for cancer therapy.

Lipid signaling in the arachidonic acid (ARA) cascade is an important therapeutic target for many human disorders (1–3). Nonsteroidal anti-inflammatory drugs (NSAIDs) and cyclooxygenase (COX)-2–selective inhibitors (coxibs), which block COX-2–mediated conversion of ARA to prostaglandin E_2 (PGE_2), are widely used to treat inflammation and pain (4). Besides the COX pathway, ARA is also a substrate of cytochrome P450 (CYP) epoxygenases (largely CYP2C and CYP2J), which convert it to epoxyeicosatrienoic acids (EETs) (3). EETs have been investigated as autocrine and paracrine mediators with antihypertensive, anti-inflammatory, analgesic, and cardioprotective effects (5). Although chemically stable, EETs are unstable in vivo due to their rapid metabolism by soluble epoxide hydrolase (sEH) to form dihydroxyeicosatrienoic acids (DHETs), which are usually less active or inactive (5). Pharmacological inhibitors of sEH (sEHIs) that stabilize endogenous EETs are currently being explored as therapeutics (6).

Our previous studies in murine models demonstrated powerful interactions of COX-2 and sEH pathways on pain and inflammation. Pharmacological inhibition of sEH or mice with global disruption of the gene that encodes sEH (sEH-null) synergized with multiple COX inhibitors (including NSAIDs, coxibs, and aspirin) to suppress inflammation and pain with reduced cardiovascular toxicity (7, 8). Due to the potent synergistic interactions, we recently designed and synthesized the first-in-class, to our knowledge, COX-2/sEH dual pharmacological inhibitors, which concurrently inhibit both COX-2 and sEH enzymes (9). A COX-2/sEH dual inhibitor, 4-(5-phenyl-3-{3-[3-(4-trifluoromethylphenyl)-ureido]-propyl}-pyrazol-1-yl)-benzenesulfonamide (PTUPB), as illustrated in Fig. S1, is more efficacious in attenuating inflammatory pain in vivo than celecoxib (a coxib) alone, *trans*-4-[4-(3-adamantan-1-yl-ureido)-cyclohexyloxy]-benzoic acid (*t*-AUCB) (a selective sEHI) alone, or the combination of both celecoxib and *t*-AUCB (9). Coadministration of COX-2 and sEH inhibitors or administration of a dual inhibitor acts to reduce proinflammatory eicosanoids, such as PGE_2, and to increase anti-inflammatory and cardioprotective eicosanoids, such as EETs (Fig. S1*B*). Together, these results support the potent interactions of these two lipid metabolism pathways.

Recent studies have demonstrated that both COX-2 and sEH play critical roles in angiogenesis and tumorigenesis (5, 10–13). Epidemiological and clinical evidence supports that COX-2 inhibitors inhibit multiple cancers (13). Contrary to the antitumor activity of COX-2 inhibitors, we and others have shown that when administered at the high dose of 10 $mg \cdot kg^{-1} \cdot d^{-1}$, sEHIs stimulate primary tumor growth and metastasis via EETs (11, 12, 14). Unexpectedly, we now demonstrate that a combination of a low-dose COX-2 inhibitor and a low-dose sEHI (3 $mg \cdot kg^{-1} \cdot d^{-1}$) synergistically inhibits primary tumor growth and metastasis. We extend this result by showing that the COX-2/sEH dual inhibitors also potently inhibit primary tumor growth and metastasis via suppressing tumor angiogenesis. These results support a key interaction of these two pathways on cancer progression.

Significance

Our study suggests that cyclooxygenase (COX)-2 and soluble epoxide hydrolase (sEH) pathways have potent synergistic antiangiogenic and anticancer activity. Dual pharmacological inhibition of COX-2 and sEH pathways may be useful in treating cancer with minimal toxicity associated with COX-2 inhibition.

Author contributions: G.Z., D.P., S.H.H., K.W.F., and B.D.H. designed research; G.Z., D.P., S.H.H., J.Y., L.M.M., H.I.W., J.-Y.L., Y.W., E.S.I., and S.T. performed research; J.Y. and K.W.F. contributed new reagents/analytic tools; G.Z., D.P., S.H.H., J.Y., M.W.K., R.H.W., K.W.F., and B.D.H. analyzed data; and G.Z., D.P., K.W.F., and B.D.H. wrote the paper.

Reviewers included: K.H., Wayne State University.

Conflict of interest statement: The sponsor (B.D.H.) and a coauthor (S.H.H.) are authors on a patent held by the University of California on the synthesis of the joint cyclooxygenase-soluble epoxide hydrolase inhibitor used as a probe in this study. The patent has not been licensed.

[1]G.Z. and D.P. contributed equally to this work.

[2]To whom correspondence should be addressed. Email: bdhammock@ucdavis.edu.

This article contains supporting information online at www.pnas.org/lookup/suppl/doi:10.1073/pnas.1410432111/-/DCSupplemental.

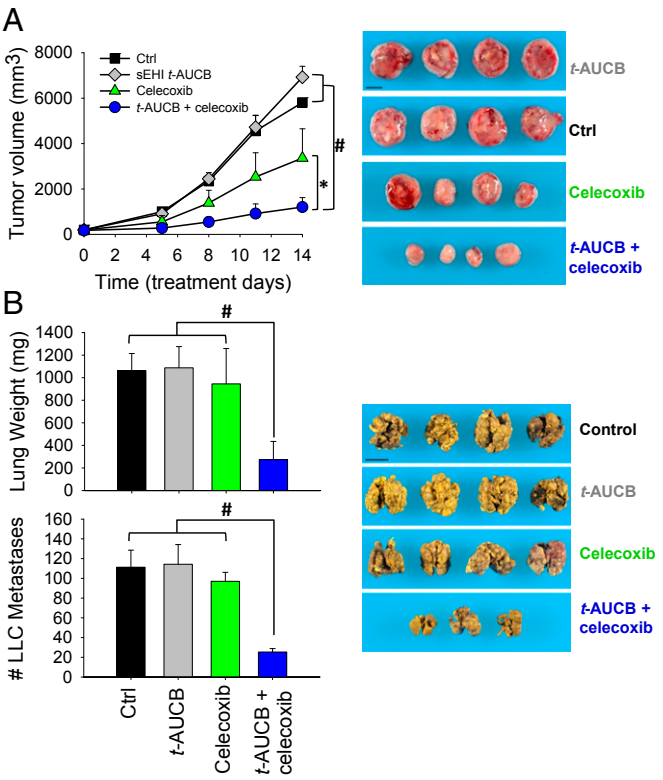

Fig. 1. Coadministration of the sEHI *t*-AUCB and celecoxib synergistically inhibits primary tumor growth and metastasis. (*A*) Coadministration of sEHI *t*-AUCB (3 mg·kg^{-1}·d^{-1}) and celecoxib (30 mg·kg^{-1}·d^{-1}) synergistically inhibited LLC growth in mice (n = 4–5 mice per group). (*B*) Coadministration of *t*-AUCB (3 mg·kg^{-1}·d^{-1}) and celecoxib (30 mg·kg^{-1}·d^{-1}) synergistically inhibited LLC metastasis in mice (n = 4–5 mice per group). (Scale bar: 1 cm.) The results are expressed as mean ± SD. *P < 0.05; #P < 0.001.

Results

Coadministration of sEHI and Coxib Suppresses Primary Tumor Growth and Metastasis. To test the interactions of sEHI and coxib on primary tumor growth and metastasis, we used a highly aggressive Lewis lung carcinoma (LLC) model in C57BL/6 mice (11). For primary tumor growth, established primary LLC tumors (100–200 mm^3) were treated with low-dose *t*-AUCB (a selective sEHI) and/or celecoxib. After 14 d of treatment, *t*-AUCB alone (3 mg·kg^{-1}·d^{-1}) had minimal activity on tumor growth, whereas celecoxib alone (30 mg·kg^{-1}·d^{-1}) inhibited tumor growth by 42%. Unexpectedly, the combination of *t*-AUCB and celecoxib markedly inhibited LLC growth by 79% (Fig. 1*A*). For tumor metastasis, we used a well-established LLC resection model in which resection of the primary LLC tumor triggers spontaneous lung metastasis due to reduced levels of circulating angiogenesis inhibitors derived from the primary tumors (11, 15, 16). Treatment with *t*-AUCB (3 mg·kg^{-1}·d^{-1}) or celecoxib (30 mg·kg^{-1}·d^{-1}) alone had no effect on LLC metastasis, whereas coadministration of both compounds resulted in a dramatic 71–74% reduction in surface metastatic foci and lung weight, a surrogate marker of metastatic burden (Fig. 1*B*). Together, these results support the potent synergistic antitumor effect of sEHI and coxib on primary tumor growth and metastasis.

Because primary tumor growth and metastasis are angiogenesis-dependent (17), we next studied whether coadministration of sEHI and coxib synergistically suppressed angiogenesis. The combination of low-dose *t*-AUCB and celecoxib synergistically inhibited endothelial cell proliferation in vitro (Fig. S2), supporting an antiangiogenic mechanism.

COX-2/sEH Dual Inhibitor PTUPB Inhibits Angiogenesis. Combination therapy is often challenging because of poor patient compliance, complicated drug–drug interactions, or patient-dependent differences in the pharmacokinetic (PK) profiles of each drug (18). To investigate the synergistic interactions of COX-2 and sEH on cancer further, we studied the role of the COX-2/sEH dual pharmacological inhibitors in angiogenesis and cancer. A dual inhibitor, PTUPB, inhibits sEH with IC_{50} = 0.9 nM, which is comparable to the selective sEHIs developed in our laboratory (19). It is a COX-2–selective inhibitor with IC_{50} = 1.26 μM for COX-2 and IC_{50} > 100 μM for COX-1, and it is more potent than rofecoxib (Vioxx) and indomethacin (Indocin) for COX-2 inhibition (9). In addition, it possesses adequate PK properties (PK data in Fig. S1*C* and Table S1); thus, we have selected PTUPB as our probe.

PTUPB inhibited endothelial tube formation (Fig. 2*A*) and aortic vessel sprouting (Fig. S3*A*) in a dose-dependent manner.

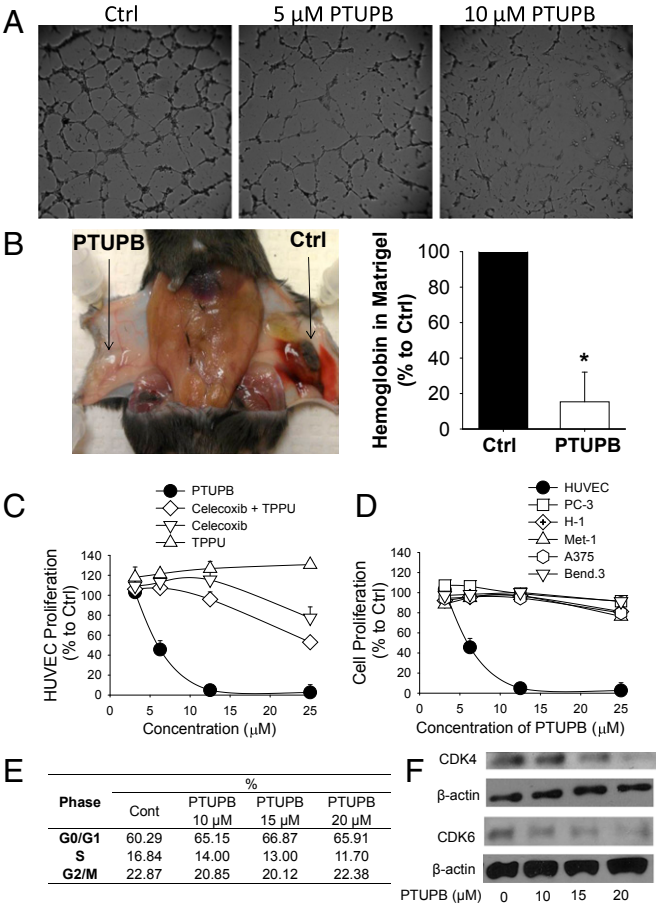

Phase	% Cont	PTUPB 10 μM	PTUPB 15 μM	PTUPB 20 μM
G0/G1	60.29	65.15	66.87	65.91
S	16.84	14.00	13.00	11.70
G2/M	22.87	20.85	20.12	22.38

Fig. 2. PTUPB inhibits angiogenesis. (*A*) PTUPB inhibits endothelial tube formation after 6 h of treatment in HUVECs. (*B*) PTUPB inhibits VEGF-induced angiogenesis in a Matrigel plug assay in C57BL/6 mice after 4 d of treatment (5.4 μg of PTUPB in 0.5 mL of Matrigel, n = 6 mice per group). (*C*) PTUPB inhibits cell proliferation in a dose-dependent manner, with higher potency than celecoxib, TPPU, or a combination of celecoxib and TPPU (1:1 molar/molar ratio) after 3 d of treatment in HUVECs. (*D*) PTUPB has minimal inhibitory effects on cell proliferation in multiple cancer cell lines [human prostate cancer (PC-3), mouse breast cancer (Met-1), and human melanoma (H-1 and A375)] and a transformed endothelial cell line (bEnd.3), whereas it potently inhibits HUVEC proliferation after 3 d of treatment. (*E*) PTUPB caused cell cycle arrest at the G0/1 phase after 24 h of treatment in HUVECs. Cont, DMSO vehicle control. (*F*) PTUPB inhibited expression of CDK4 and CDK6 in a dose-dependent manner after 24 h of treatment in HUVECs. The results are expressed as mean ± SD. *P < 0.05. Ctrl, control.

In a Matrigel (BD Biosciences) plug assay in mice (20), PTUPB inhibited VEGF-induced angiogenesis by 85% after 4 d of treatment (Fig. 2*B*). Thus, PTUPB is antiangiogenic in vitro and in vivo. The process of angiogenesis involves multiple cellular steps, including endothelial cell migration, proliferation, and production of matrix metalloproteinases (MMPs) (21). Therefore, we further characterized the antiangiogenic activity of PTUPB. PTUPB had no effect on endothelial cell migration or MMP activity (Fig. S3 *B–D*), although it specifically inhibited endothelial cell proliferation more potently than celecoxib alone, 1-trifluoromethoxyphe-nyl-3-(1-propionylpiperidin-4-yl)urea (TPPU, a selective sEHI) alone, or a combination of both (Fig. 2*C*). Interestingly, PTUPB had minimal inhibitory activity on cancer cell proliferation, including human prostate cancer (PC-3), human melanoma (H-1 and A375), and mouse breast cancer (Met-1), as well as a transformed endothelial cell line (bEnd.3), after a 3 d of treatment (Fig. 2*D*). This conclusion was further supported by a National Cancer Institute-60 human cancer cell line screening showing that PTUPB had minimal inhibitory effects on cell proliferation in most of the 60 human cancer cell lines (Fig. S4*A*). Besides PTUPB, other dual inhibitors synthesized also specifically inhibited endothelial cell proliferation (Fig. S4 *B* and *C*).

Because VEGF receptor 2 (VEGFR2) is a critical mediator of angiogenesis and cancer (22, 23), we studied whether PTUPB inhibited angiogenesis via a VEGFR2-dependent mechanism. PTUPB at 10 μM had no inhibition not only on VEGFR2 kinase activity in a cell-free VEGFR2 kinase assay (Fig. S4*D*) but also on VEGF-induced VEGFR2 phosphorylation in human umbilical vein endothelial cells (HUVECs) (Fig. S4*E*), suggesting

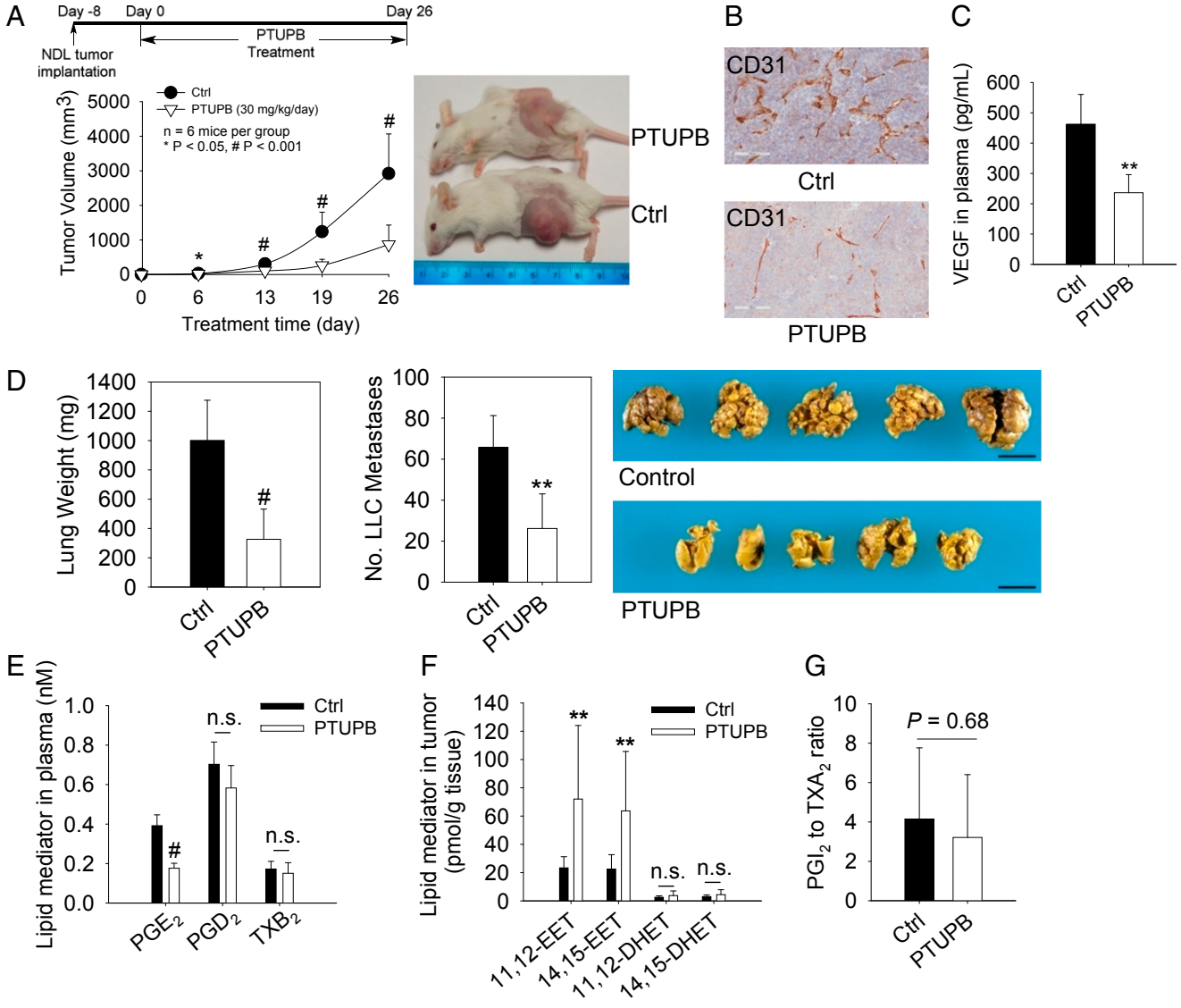

Fig. 3. PTUPB inhibits primary tumor growth and metastasis. (*A*) PTUPB inhibits NDL breast tumor growth in FVB female mice ($n = 6$ mice per group). Experimental design (*Upper Left*), time course of NDL tumor growth (*Lower Left*), and representative images of mice on day 26 (*Right*). (*B*) PTUPB reduces CD31-positive endothelium in NDL tumors. (*C*) PTUPB reduces the circulating level of VEGF. (*D*) PTUPB inhibits LLC metastasis ($n = 5$–7 mice per group). PTUPB reduces lung tissue weight (*Left*) and suppresses LLC metastasis (*Center*); representative images of spontaneous lung metastasis are shown (*Right*). (Scale bar: 1 cm.) (*E*) PTUPB reduces the level of PGE_2 in plasma in the NDL tumor experiments. n.s., not significant. (*F*) PTUPB increases levels of 11,12-EET and 14,15-EET in tumors. (*G*) PTUPB does not alter the ratio of PGI_2 (stable metabolite 6-keto-$PGF_{1\alpha}$) to TXA_2 (stable metabolite TXB_2) in plasma. The results are expressed as mean ± SD. *$P < 0.05$; **$P < 0.01$; #$P < 0.001$.

that PTUPB does not inhibit angiogenesis by altering VEGFR2 signaling.

Because PTUPB inhibited endothelial cell proliferation, we analyzed the effect of PTUPB on cell cycle in endothelial cells. Cell cycle analysis showed that PTUPB induced cell cycle arrest at the G0/1 phase (Fig. 2*E*). Cyclin D1 and cyclin-dependent kinase 4 (CDK4) or cyclin-dependent kinase 6 (CDK6) complex promotes the G1-S transition, whereas p53 family proteins, including p21 and p27, whose transcription is regulated by p53, inhibit the G1-S transition by binding the complexes (24). PTUPB at 10–20 μM attenuated levels of CDK4 and CDK6 proteins in a dose-dependent manner after a 24-h treatment in HUVECs (Fig. 2*F*), whereas cyclin D1 and p53 levels were not affected (Fig. S4*F*), demonstrating that PTUPB caused cell cycle arrest at the G0/1 phase via inhibition of CDK4 and CDK6.

COX-2/sEH Dual Inhibitor PTUPB Inhibits Primary Tumor Growth and Metastasis. For primary tumor growth, dual inhibition of COX-2 and sEH by systematic administration of 30 $mg{\cdot}kg^{-1}{\cdot}d^{-1}$ of PTUPB inhibited NDL and LLC tumor growth by 70–83% (Fig. 3*A* and Fig. S5*A*). PTUPB exhibited no overt toxicity, such as any weight loss, compared with the control group (Fig. S5*B*). PTUPB treatment significantly suppressed CD31-positive endothelium in NDL tumors and the plasma level of VEGF (Fig. 3 *B* and *C*), demonstrating that PTUPB inhibits tumor angiogenesis. To study tumor metastasis, we used the primary tumor (LLC) resection metastasis model (11, 15, 16). PTUPB treatment for 14 d resulted in potent suppression of surface metastatic foci and lung weight by 61–67% (Fig. 3*D*). The efficacy of PTUPB on inhibition of primary tumor growth and metastasis is comparable to the coadministration of celecoxib and *t*-AUCB in the LLC model (Fig. 1). The dose of PTUPB in the tumor experiments was determined to be 30 $mg{\cdot}kg^{-1}{\cdot}d^{-1}$ on the basis of a dose–response PK study, which showed that at a dose of ∼30 mg/kg, the peak plasma concentration of PTUPB was above its IC_{50} value for COX-2 (Fig. S1*C* and Table S1).

Pharmacological Target Engagement of Dual Inhibitor PTUPB. To test whether inhibition of COX-2 and sEH pathways is involved in the mode of action of PTUPB in vivo, we analyzed eicosanoid profiles using LC-tandem MS–based lipidomics (25). PTUPB treatment reduced PGE_2 in plasma by ∼55% ($P < 0.001$), indicating that PTUPB inhibited the COX-2 pathway in vivo (Fig. 3*E*). For the CYP/sEH pathway, PTUPB treatment caused an approximately threefold increase of 11,12-EET and 14,15-EET in NDL tumors, whereas it had no effect on the corresponding diol metabolites 11,12-DHET and 14,15-DHET (Fig. 3*F*). PTUPB increased the ratio of 5,6-EET to its sEH metabolite 5,6-DHET by 43% and the ratio of 10,11-epoxydocosapentaenoic acid (EDP) to its sEH metabolite 10,11-dihydroxydocosapentaenoic acid (DiHDPA) by 97% in plasma (Fig. S6). Together, these results indicate that PTUPB inhibited the sEH pathway in vivo. The lipid mediators from other pathways were not significantly changed (Table S2). Together, these data support that PTUPB inhibits both COX-2 and sEH, although it may have effects on other cellular targets.

A major theory to explain the potential cardiovascular risks of coxibs is that they block the formation of prostacyclin (PGI_2), which is a potent vasodilator, but not COX-1–derived thromboxane A_2 (TXA_2), which is a potent vasoconstrictor; therefore, a decrease of the PGI_2-to-TXA_2 ratio may increase the incidence of thrombotic cardiovascular events (26). Consistent with this theory, our previous study showed that a 6-h treatment with either celecoxib or rofecoxib significantly reduced the ratio of PGI_2 [by measuring its stable metabolite 6-keto prostaglandin $F_{1\alpha}$ (6-keto-$PGF_{1\alpha}$)] to TXA_2 (by measuring its stable metabolite TXB_2) in plasma in mice (7). Even though PTUPB is also a selective COX-2 inhibitor (IC_{50} for COX-2 = 1.26 μM, IC_{50} for COX-1 > 100 μM), the ratio of PGI_2 to TXA_2 in plasma was not significantly altered after a 26-d treatment with PTUPB (Fig. 3*G*), suggesting that PTUPB may have reduced cardiovascular risks compared with coxibs, such as celecoxib or rofecoxib.

Discussion

COX inhibitors and sEHIs reduce inflammation and pain (4, 27, 28). We previously demonstrated that a combination of sEHIs [such as 12-(3-adamantan-1-yl-ureido)-dodecanoic acid *n*-butyl ester (AUDA-nBE) or *t*-AUCB] and COX inhibitors (indomethacin, celecoxib, rofecoxib, or aspirin) synergistically inhibited LPS-induced inflammation and pain in mice (7, 8). Studies in sEH-null mice also show that interaction with aspirin suppresses LPS-induced inflammation and hypotension (8). These results support the potent interactions of these two pathways. One possible mechanism to explain the interactions of COX-2 and sEH pathways is a reduction of PGE_2. In an LPS-induced murine inflammation model, we have shown that coadministration of sEHI and COX inhibitors dramatically reduced circulating PGE_2 (7, 8). The reduction of PGE_2 is likely due to both inhibition of COX-2 transcription by sEH inhibition and inhibition of COX-2 enzymatic activity by COX inhibitors (29). PGE_2 has potent proangiogenic, proinflammatory, and protumorigenic effects (13); therefore, a dramatic reduction of PGE_2 may, in part, mediate the effects of the dual inhibition of sEH and COX-2.

We previously demonstrated that high-dose sEHI *t*-AUCB (10 $mg{\cdot}kg^{-1}{\cdot}d^{-1}$) increased primary tumor growth and metastasis by stimulating tumor angiogenesis and VEGF levels (11) but low-dose *t*-AUCB (1 $mg{\cdot}kg^{-1}{\cdot}d^{-1}$) inhibited LLC metastasis by 31% ($P = 0.057$) (12). We now show that *t*-AUCB alone at 3 $mg{\cdot}kg^{-1}{\cdot}d^{-1}$ has no effect on primary tumor growth and metastasis. Importantly, the combination of low-dose sEHI *t*-AUCB and the COX-2 inhibitor celecoxib synergistically suppresses primary tumor growth and metastasis. Our primary tumor and metastasis studies with the COX-2/sEH dual inhibitor PTUPB further supported these results. It appears that sEH inhibition or EETs have biphasic dose-dependent activity on angiogenesis, primary tumor growth, and metastasis. In fact, several angiogenesis modulators, such as α-IFN, endostatin, rosiglitazone, statins, chemotherapy (e.g., 5-fluorouracil, cisplatinum), bortezomib, enterostatin, integrin inhibitors, plasminogen activator-1, rapamycin, thrombospondin-1, TGF-α1, and TGF-α3, have been shown to exhibit a biphasic, U-shaped, or J-shaped dose-efficacy curve known as hormesis (16, 17, 30–34). The sEHIs may be an addition to this growing class of angiogenesis modulators that exhibit a hormesis response. Coxibs have anti-inflammatory and antiangiogenic activity on tumor growth (13). Low-dose sEHIs may further sensitize the anti-inflammatory and antiangiogenic effects of COX-2 inhibition. Our previous studies, as well as those of others, have demonstrated that the proangiogenic and protumorigenic effects of EETs require VEGF. For example, blocking the VEGF pathway abolishes the proangiogenic and protumorigenic effects of EETs (11, 35–37). COX-2 inhibition has been shown to inhibit VEGF production (38); thus, coinhibition of COX-2 may reduce or eliminate the proangiogenic effects of EETs. As expected here, we also found that PTUPB reduced the plasma VEGF level by 50%. The reduction of VEGF and PGE_2 and the stabilization of anti-inflammatory EETs are consistent with the observed effects.

Importantly, we show that COX-2/sEH dual inhibitors are selective inhibitors of endothelial cell proliferation. We screened over 60 different cell lines and found that only HUVECs (a primary endothelial cell line) were highly sensitive to the antiproliferative effect of PTUPB. Few such selective inhibitors of endothelial proliferation have been discovered; other examples include TNP-470 (39), rosiglitazone (16), cytochalasin E (40) and cortistatin A (41). TNP-470 is, to our knowledge, the first synthetic angiogenesis inhibitor to be discovered, and it has been

intensively characterized (39). Similar to PTUPB, TNP-470 is a potent inhibitor of cell proliferation in primary endothelial cells, but it does not inhibit proliferation of transformed endothelial cells or cancer cells (42). TNP-470 inhibited endothelial cell proliferation via cell cycle arrest at the G1 phase (42); however, the mechanism by which it selectively inhibits endothelial cell proliferation is not well understood (43, 44). Here, we find that PTUPB arrested the cell cycle at the G0/1 phase via a mechanism involving inhibition of CDK4 and CDK6 in HUVECs and that it did not inhibit VEGFR2 signaling.

The COX-2/sEH dual inhibitors were designed and optimized using in vitro enzymatic assays of COX-1, COX-2, and sEH (9). Here, we provide in vivo evidence that systematic administration of PTUPB decreased PGE_2 and increased EETs (and other fatty acid epoxides) in mice, with minimal alteration of other lipid mediators, supporting the pharmacological targets by the selective dual inhibition of both COX-2 and sEH. An early sepsis study showed that in addition to the expected changes in the P450 metabolites, inflammatory COX-derived metabolites were reduced by the sEHIs. At higher doses, the sEHIs also reduced inflammatory lipoxygenase (LOX)-derived metabolites (27). In an LPS-induced inflammation and pain model, inhibition of sEH reduced levels of LOX, as well as P450 and COX metabolites. This reduction in pain and inflammation was enhanced by coinhibition of the 5-LOX pathway (8). However, using lower doses of sEHIs, we did not observe changes in LOX metabolites. Dual inhibition with low doses of COX-2 and sEHIs synergistically inhibited COX-2–derived eicosanoids, such as PGE_2, but did not alter LOX metabolites (7, 8). Thus, it was not surprising that the low-dose dual inhibitor PTUPB used in this study did not alter the levels of LOX-derived eicosanoids in plasma and tumor tissues. Although we show that PTUPB inhibits COX-2 and sEH, it may have other targets. Looking forward, the chemical scaffold of PTUPB provides a starting point for further structural modification of COX-2/sEH dual inhibitors to optimize its PK profile (9). Due to its poor oral bioavailability, we continuously infused PTUPB into mice in tumor experiments using an osmotic minipump to test the concept of dual inhibition of COX-2 and sEH. Further structural optimization using medicinal chemistry could improve its PK profile for oral administration. In addition, if inhibition of both COX-1 and COX-2 enzymes is required, these properties could be designed into the molecule. PTUPB is a dramatically more potent sEHI than COX-2 inhibitor. Some selectivity in favor of sEH is desirable because complete inhibition of an enzyme degrading an apparently beneficial lipid mediator is attractive (5). Also, the sEHIs studied to date appear to have a massive therapeutic index compared with a more limited one with COX inhibitors (19). More potent COX inhibition may be desirable; however, this could be challenging because in vitro COX assays correlate weakly with in vivo efficacy (4) and PTUPB is already more potent than many marketed NSAIDs and coxibs for COX-2 inhibition (9).

In conclusion, our study suggests that COX-2 and sEH pathways have potent interactions on angiogenesis and cancer. Dual pharmacological inhibition of COX-2 and sEH pathways is a promising therapeutic approach to treating cancer with minimal toxicity.

Materials and Methods

Details of the experimental protocols are given in *SI Materials and Methods*.

Primary Tumor Growth. For the LLC primary tumor model, LLC cells (1 million cells per mouse) were s.c. injected into C57BL/6 mice. When the tumor size reached 200 mm^3, the mice were treated with *t*-AUCB (3 $mg{\cdot}kg^{-1}{\cdot}d^{-1}$) and/or celecoxib (30 $mg{\cdot}kg^{-1}{\cdot}d^{-1}$) by oral gavage ($n$ = 4–5 mice per group, drugs were dissolved in 0.45% methylcellulose). Tumor sizing was measured by a caliper. For the NDL tumor model, NDL breast tumor pieces (1 mm^3) were transplanted into the fourth inguinal mammary fat pads of FVB female mice. After 8 d of tumor implantation, the mice were randomized to two groups (n = 6 mice per group) and treated with PTUPB (30 $mg{\cdot}kg^{-1}{\cdot}d^{-1}$) dissolved in a mixed solvent of PEG 400 and DMSO (1:1 vol/vol) or vehicle control (PEG 400 and DMSO, 1:1 vol/vol) using Alzet osmotic minipumps (model 2004; DURECT Corporation) for 4 wk. During this period, the changes in tumor growth were checked by ultrasound imaging (Acuson Sequoia 512; Siemens). At the end of the experiment, the plasma was collected for lipid mediator analysis. Tumor angiogenesis was analyzed by immunohistochemistry using CD31 and H&E staining. Plasma VEGF was measured using ELISA (VEGF Mouse ELISA Kit; Invitrogen).

Tumor Metastasis. LLC cells (1 million cells per mouse) were injected s.c. into 6-wk old male C57BL6 mice. At 23 d after injection of LLC cells (when LLC tumors are 2–4 cm^3), LLC tumors were resected and PTUPB or vehicle pumps were implanted. The mice were euthanized on day 14 postresection, and lungs were evaluated for weight and number of surface metastases as described (11, 15, 16).

Statistics. Group comparisons were carried out using one-way ANOVA or the Student *t* test. A P value less than 0.05 was considered statistically significant. Data are presented as mean ± SD.

ACKNOWLEDGMENTS. This study was supported by National Institute of Environmental Health Sciences Grant R01 ES02710 and Superfund P42 ES04699 and National Institutes of Health/National Institute for Occupational Safety and Health Grant U54 OH07550 (to B.D.H.); by Grants R01 CA134659, R01 CA112356, and R01 CA103828 (to K.W.F.), National Heart, Lung and Blood Institute Contract no. HHSN268201000043 (to K.W.F.), and the Research Investments in the Sciences and Engineering Program of the University of California, Davis (K.W.F.); by Grant R01 CA148633 (to D.P.); by the Stop and Shop Pediatric Brain Tumor Fund and the C. J. Buckley Pediatric Brain Tumor Fund (M.W.K.); and by Grants R01 CA135401 and R01 DK082690 (to R.H.W.) and the Medical Service of the Department of Veterans Affairs (R.H.W.). B.D.H. is a George and Judy Marcus Senior Fellow of the American Asthma Society.

1. Buczynski MW, Dumlao DS, Dennis EA (2009) Thematic Review Series: Proteomics. An integrated omics analysis of eicosanoid biology. *J Lipid Res* 50(6):1015–1038.
2. Funk CD (2001) Prostaglandins and leukotrienes: Advances in eicosanoid biology. *Science* 294(5548):1871–1875.
3. Zeldin DC (2001) Epoxygenase pathways of arachidonic acid metabolism. *J Biol Chem* 276(39):36059–36062.
4. Marnett LJ (2009) The COXIB experience: A look in the rearview mirror. *Annu Rev Pharmacol Toxicol* 49(1):265–290.
5. Zhang G, Kodani S, Hammock BD (2014) Stabilized epoxygenated fatty acids regulate inflammation, pain, angiogenesis and cancer. *Prog Lipid Res* 53(0):108–123.
6. Imig JD, Hammock BD (2009) Soluble epoxide hydrolase as a therapeutic target for cardiovascular diseases. *Nat Rev Drug Discov* 8(10):794–805.
7. Schmelzer KR, et al. (2006) Enhancement of antinociception by coadministration of nonsteroidal anti-inflammatory drugs and soluble epoxide hydrolase inhibitors. *Proc Natl Acad Sci USA* 103(37):13646–13651.
8. Liu JY, et al. (2010) Inhibition of soluble epoxide hydrolase enhances the anti-inflammatory effects of aspirin and 5-lipoxygenase activation protein inhibitor in a murine model. *Biochem Pharmacol* 79(6):880–887.
9. Hwang SH, et al. (2011) Synthesis and structure-activity relationship studies of urea-containing pyrazoles as dual inhibitors of cyclooxygenase-2 and soluble epoxide hydrolase. *J Med Chem* 54(8):3037–3050.
10. Panigrahy D, et al. (2013) Epoxyeicosanoids promote organ and tissue regeneration. *Proc Natl Acad Sci USA* 110(33):13528–13533.
11. Panigrahy D, et al. (2012) Epoxyeicosanoids stimulate multiorgan metastasis and tumor dormancy escape in mice. *J Clin Invest* 122(1):178–191.
12. Zhang G, et al. (2013) Epoxy metabolites of docosahexaenoic acid (DHA) inhibit angiogenesis, tumor growth, and metastasis. *Proc Natl Acad Sci USA* 110(16):6530–6535.
13. Wang D, Dubois RN (2010) Eicosanoids and cancer. *Nat Rev Cancer* 10(3):181–193.
14. Skrypnyk N, et al. (2014) PPARα activation can help prevent and treat non-small cell lung cancer. *Cancer Res* 74(2):621–631.
15. O'Reilly MS, et al. (1994) Angiostatin: A novel angiogenesis inhibitor that mediates the suppression of metastases by a Lewis lung carcinoma. *Cell* 79(2):315–328.
16. Panigrahy D, et al. (2002) PPARgamma ligands inhibit primary tumor growth and metastasis by inhibiting angiogenesis. *J Clin Invest* 110(7):923–932.
17. Folkman J (2007) Angiogenesis: An organizing principle for drug discovery? *Nat Rev Drug Discov* 6(4):273–286.
18. Morphy R, Rankovic Z (2005) Designed multiple ligands. An emerging drug discovery paradigm. *J Med Chem* 48(21):6523–6543.
19. Shen HC, Hammock BD (2012) Discovery of inhibitors of soluble epoxide hydrolase: A target with multiple potential therapeutic indications. *J Med Chem* 55(5):1789–1808.

20. Adini A, et al. (2009) Matrigel cytometry: A novel method for quantifying angiogenesis in vivo. *J Immunol Methods* 342(1-2):78–81.
21. Griffioen AW, Molema G (2000) Angiogenesis: Potentials for pharmacologic intervention in the treatment of cancer, cardiovascular diseases, and chronic inflammation. *Pharmacol Rev* 52(2):237–268.
22. Ferrara N, Gerber HP, LeCouter J (2003) The biology of VEGF and its receptors. *Nat Med* 9(6):669–676.
23. Koch S, Claesson-Welsh L (2012) Signal transduction by vascular endothelial growth factor receptors. *Cold Spring Harb Perspect Med* 2(7):a006502.
24. Musgrove EA, Caldon CE, Barraclough J, Stone A, Sutherland RL (2011) Cyclin D as a therapeutic target in cancer. *Nat Rev Cancer* 11(8):558–572.
25. Yang J, Schmelzer K, Georgi K, Hammock BD (2009) Quantitative profiling method for oxylipin metabolome by liquid chromatography electrospray ionization tandem mass spectrometry. *Anal Chem* 81(19):8085–8093.
26. Cheng Y, et al. (2002) Role of prostacyclin in the cardiovascular response to thromboxane A2. *Science* 296(5567):539–541.
27. Schmelzer KR, et al. (2005) Soluble epoxide hydrolase is a therapeutic target for acute inflammation. *Proc Natl Acad Sci USA* 102(28):9772–9777.
28. Node K, et al. (1999) Anti-inflammatory properties of cytochrome P450 epoxygenase-derived eicosanoids. *Science* 285(5431):1276–1279.
29. Panigrahy D, Greene ER, Pozzi A, Wang DW, Zeldin DC (2011) EET signaling in cancer. *Cancer Metastasis Rev* 30(3-4):525–540.
30. Tjin Tham Sjin RM, et al. (2006) Endostatin therapy reveals a U-shaped curve for antitumor activity. *Cancer Gene Ther* 13(6):619–627.
31. Slaton JW, Perrotte P, Inoue K, Dinney CP, Fidler IJ (1999) Interferon-α-mediated down-regulation of angiogenesis-related genes and therapy of bladder cancer are dependent on optimization of biological dose and schedule. *Clin Cancer Res* 5(10):2726–2734.
32. Reynolds AR (2009) Potential relevance of bell-shaped and u-shaped dose-responses for the therapeutic targeting of angiogenesis in cancer. *Dose Response* 8(3):253–284.
33. Celik I, et al. (2005) Therapeutic efficacy of endostatin exhibits a biphasic dose-response curve. *Cancer Res* 65(23):11044–11050.
34. Calabrese EJ, Staudenmayer JW, Stanek EJ (2006) Drug development and hormesis: Changing conceptual understanding of the dose response creates new challenges and opportunities for more effective drugs. *Curr Opin Drug Discov Devel* 9(1):117–123.
35. Cheranov SY, et al. (2008) An essential role for SRC-activated STAT-3 in 14,15-EET-induced VEGF expression and angiogenesis. *Blood* 111(12):5581–5591.
36. Webler AC, et al. (2008) Epoxyeicosatrienoic acids are part of the VEGF-activated signaling cascade leading to angiogenesis. *Am J Physiol Cell Physiol* 295(5): C1292–C1301.
37. Yang S, Wei S, Pozzi A, Capdevila JH (2009) The arachidonic acid epoxygenase is a component of the signaling mechanisms responsible for VEGF-stimulated angiogenesis. *Arch Biochem Biophys* 489(1-2):82–91.
38. Wu G, et al. (2006) Involvement of COX-2 in VEGF-induced angiogenesis via P38 and JNK pathways in vascular endothelial cells. *Cardiovasc Res* 69(2):512–519.
39. Ingber D, et al. (1990) Synthetic analogues of fumagillin that inhibit angiogenesis and suppress tumour growth. *Nature* 348(6301):555–557.
40. Udagawa T, et al. (2000) Cytochalasin E, an epoxide containing Aspergillus-derived fungal metabolite, inhibits angiogenesis and tumor growth. *J Pharmacol Exp Ther* 294(2):421–427.
41. Aoki S, et al. (2007) Structure-activity relationship and biological property of cortistatins, anti-angiogenic spongean steroidal alkaloids. *Bioorg Med Chem* 15(21): 6758–6762.
42. Antoine N, et al. (1994) AGM-1470, a potent angiogenesis inhibitor, prevents the entry of normal but not transformed endothelial cells into the G1 phase of the cell cycle. *Cancer Res* 54(8):2073–2076.
43. Zhang Y, Griffith EC, Sage J, Jacks T, Liu JO (2000) Cell cycle inhibition by the anti-angiogenic agent TNP-470 is mediated by p53 and p21WAF1/CIP1. *Proc Natl Acad Sci USA* 97(12):6427–6432.
44. Yeh JR, Mohan R, Crews CM (2000) The antiangiogenic agent TNP-470 requires p53 and p21CIP/WAF for endothelial cell growth arrest. *Proc Natl Acad Sci USA* 97(23): 12782–12787.